

Asymptotic Behavior of Generalized Partial Directed Coherence

Carlos Stein Naves de Brito Luiz Antonio Baccalá Daniel Yasumasa Takahashi Koichi Sameshima

Abstract—This paper examines the asymptotic behavior of a newly defined general form of partial directed coherence. Both confidence interval and null hypothesis testing results are presented and illustrated.

I. INTRODUCTION

In [1] we introduced the notion of *partial directed coherence* (PDC) as a means of evaluating the connectivity between neural structures. PDC is a multivariate time series technique obtained from the factorization of partial coherence (see [2]), which in the frequency domain closely reflects the idea of Granger causality[3], i.e. that a time series $x(k)$ is Granger caused by $y(k)$ only if knowledge of $y(k)$'s past proves helpful in predicting $x(k)$. One should stress that PDC's representation of Granger causality in the frequency domain is important since many neuroscience research scenarios, like sleep staging for example [4], have long been known to be characterized by typical oscillatory neuro electrical signal behavior.

Though PDC has been finding increasing applications, [5], [6], [7], most of it has been carried out by comparing sample connectivities between groups classified as presenting some known disorder against normal controls. It was only recently, however, that objective trial by trial criteria have appeared that allow estimating rigorous asymptotic properties of the PDC estimator. In [8] previously available connectivity hypothesis tests were rigorously confirmed and hitherto unavailable PDC confidence intervals were derived.

This scenario has recently been compounded by the introduction of other more general expressions for PDC which can be more adequate under certain special circumstances. One such case is that of what we called generalized PDC (*gPDC*) [9], which is better suited to the analysis of cases of large prediction errors or power spectra disparity between the multivariate channels.

The aim of this paper is to extend the methodology of [8] to the above more general form of PDC. The presentation is organized as follows: In Sec. II we briefly review PDC and its generalized form. This is followed by a concise statement of the asymptotic mathematical results in Sec. III

which is numerically illustrated in Sec. IV topped by a brief discussion in Sec. V.

II. BACKGROUND

The point of departure for defining PDC and its variants is an adequately fitted multivariate autoregressive time series (i.e. vector time series) model

$$\mathbf{x}(n) = \sum_{r=1}^p \mathbf{A}(r)\mathbf{x}(n-r) + \mathbf{w}(n) \quad (1)$$

to which a multivariate signal $\mathbf{x}(n)$ made up by $x_k(n)$, $k = 1 \dots, K$ simultaneously acquired time series conform and where $\mathbf{w}(n)$ stands for a zero mean white innovation process of with $\Sigma_w = [\sigma_{ij}]$ as its covariance matrix and p is the model order. The coefficients $a_{ij}(r)$ composing each $\mathbf{A}(r)$ matrix describe the lagged effect of the the j -th series on the i -th series, wherefrom one can also define a frequency domain representation of (1) via the $\bar{\mathbf{A}}(\lambda)$ matrix whose entries are given by

$$\bar{A}_{ij}(\lambda) = \begin{cases} 1 - \sum_{r=1}^p a_{ij}(r)e^{-j2\pi\lambda r}, & \text{if } i = j \\ - \sum_{r=1}^p a_{ij}(r)e^{-j2\pi\lambda r}, & \text{otherwise} \end{cases} \quad (2)$$

where $\mathbf{j} = \sqrt{-1}$, which allows writing *gPDC* [9] as

$$g\pi_{ij}(\lambda) = \frac{\frac{1}{\sigma_{ii}^{1/2}} \bar{A}_{ij}(\lambda)}{\sqrt{\sum_{k=1}^K \frac{1}{\sigma_{kk}} |\bar{A}_{kj}(\lambda)|^2}}. \quad (3)$$

A. Problem Formulation

In [8] we addressed the asymptotic behavior of the original unnormalized PDC when testing for its nullity (i.e. conditions of asymptotic connectivity rejection) and when obtaining confidence intervals in the case of statistically significant connectivity.

To that end, the delta method [10] was applied to (3) rewritten as a ratio of real quadratic forms in the $a_{ij}(r)$ parameters by the same approach as in [8] where an adequate rearrangement of the coefficients in (1) as

$$\boldsymbol{\alpha} = \text{vec}[\mathbf{A}(1) \mathbf{A}(2) \dots \mathbf{A}(p)]$$

allows jointly expressing (2) as real-valued vector:

$$\boldsymbol{\alpha}(\lambda) = \begin{bmatrix} \text{vec}(\text{Re}(\bar{\mathbf{A}}(\lambda))) \\ \text{vec}(\text{Im}(\bar{\mathbf{A}}(\lambda))) \end{bmatrix} = \begin{bmatrix} \text{vec}(\mathcal{I}_{pK^2}) \\ \mathbf{0} \end{bmatrix} - \mathcal{C}(\lambda)\boldsymbol{\alpha}$$

C. S. N. de Brito is with the Bioinformatics Graduate Program, University of São Paulo, Brazil cstein06@gmail.com

D. Y. Takahashi is with the Institute of Mathematics and Statistics, University of São Paulo, Brazil yasumasa@ime.usp.br

L. A. Baccalá is with the Telecommunications and Control Department of Escola Politécnica, University of São Paulo, São Paulo, Brazil, 05508-900 baccala@lcs.poli.usp.br

K. Sameshima is with the Department of Radiology, Faculdade de Medicina, University of São Paulo, São Paulo, Brazil, 01246-903 ksameshi@usp.br

where

$$\mathcal{C}(\lambda) = \begin{bmatrix} \mathbf{C}(\lambda) \\ -\mathbf{S}(\lambda) \end{bmatrix},$$

whose blocks are $K^2 \times pK^2$ dimensional of the form

$$\mathbf{C}(\lambda) = [\mathbf{C}_1(\lambda) \dots \mathbf{C}_p(\lambda)]$$

and

$$\mathbf{S}(\lambda) = [\mathbf{S}_1(\lambda) \dots \mathbf{S}_p(\lambda)],$$

for

$$\mathbf{C}_r(\lambda) = \text{diag}([\cos(2\pi r\lambda) \dots \cos(2\pi r\lambda)])$$

and

$$\mathbf{S}_r(\lambda) = \text{diag}([\sin(2\pi r\lambda) \dots \sin(2\pi r\lambda)]).$$

To rewrite (3) consider the following $K^2 \times K^2$ matrices:

- 1) \mathbf{I}_{ij} whose entries are zero except for indices of the form $(l, m) = ((j-1)K + i, (j-1)K + i)$, which equal 1;
- 2) \mathbf{I}_j , which is non zero only for entries whose indices are of the form $(l, m) : (j-1)K + 1 \leq l = m \leq jK$.

These matrices can be used to construct

$$\mathbf{I}_{ij}^c = \begin{bmatrix} \mathbf{I}_{ij} & 0 \\ 0 & \mathbf{I}_{ij} \end{bmatrix}$$

and

$$\mathbf{I}_j^c = \begin{bmatrix} \mathbf{I}_j & 0 \\ 0 & \mathbf{I}_j \end{bmatrix}$$

so that the general form of the absolute value of squared gPDC can be written as a ratio of quadratic forms:

$$|g\pi_{ij}(\lambda)|^2 = \frac{\mathbf{a}(\lambda)^T \mathbf{I}_{ij}^c \mathbf{S}^{-1} \mathbf{I}_{ij}^c \mathbf{a}(\lambda)}{\mathbf{a}(\lambda)^T \mathbf{I}_j^c \mathbf{S}^{-1} \mathbf{I}_j^c \mathbf{a}(\lambda)}, \quad (4)$$

where $\mathbf{S} = \mathcal{I}_{2K} \otimes (\boldsymbol{\Sigma}_w \odot \mathcal{I}_K)$ and \odot and \otimes stand for the Hadamard and Kronecker products, respectively.

III. ASYMPTOTIC RESULTS

The delta method [10] refers to the behavior of transformed statistics and takes advantage of the continuity of the transforming functions. This allows Taylor series expansions in the original variables and the number of available observations n_s . Usually only the first derivative is enough. This is the case when obtaining confidence intervals (see Sec. III-A). However, when the first derivative vanishes identically, as happens under the hypothesis of $|g\text{PDC}|^2$ nullity, the next order derivative must be computed and leads to a non-Gaussian distribution for the resulting transformed statistic (see Sec. III-B).

Before proceeding, it is worth introducing some further notation to allow writing the results compactly.

The results in Secs. III-A and III-B rest on two basic statistical facts regarding the (1)'s model parameter estimators which are [11]:

- 1) Asymptotically Gaussian

$$\sqrt{n_s}(\hat{\boldsymbol{\alpha}} - \boldsymbol{\alpha}) \rightarrow \mathcal{N}(0, \boldsymbol{\Omega}_\alpha) \quad (5)$$

where $\boldsymbol{\Omega}_\alpha = \boldsymbol{\Gamma}_x^{-1} \otimes \boldsymbol{\Sigma}_w$, with $\boldsymbol{\Gamma}_x = E[\bar{\mathbf{x}}(n)\bar{\mathbf{x}}^T(n)]$ for

$$\bar{\mathbf{x}}(n) = [x_1(n) \dots x_K(n) \dots x_1(n-p+1) \dots x_K(n-p+1)]^T; \quad (6)$$

and

- 2) Independent from the estimated innovation noise covariances, which are also normal, i.e.

$$\sqrt{n_s}(\hat{\boldsymbol{\epsilon}} - \boldsymbol{\epsilon}) \rightarrow \mathcal{N}(0, \boldsymbol{\Omega}_\epsilon), \quad (7)$$

where $\boldsymbol{\epsilon} = \text{vec}(\boldsymbol{\Sigma}_w)$ and $\boldsymbol{\Omega}_\epsilon = 2\mathbf{D}_K \mathbf{D}_K^+ (\boldsymbol{\Sigma}_w \otimes \boldsymbol{\Sigma}_w) \mathbf{D}_K^{+T} \mathbf{D}_K^T$ for \mathbf{D}^+_{+K} standing for the Moore-Penrose pseudo-inverse of the standard duplication matrix [11].

A. Confidence Intervals

Since $|g\pi_{ij}(\lambda)|^2$ is a real differentiable function of $\boldsymbol{\alpha}$ and $\boldsymbol{\epsilon}$, which conform, respectively, to (5) and (7), application of the delta method produces a normally distributed transformed variable whose covariance is obtained by weighing the original parameters by the gPDC's local first derivative.

Hence, omitting the explicit frequency λ dependence to simplify notation, the confidence interval results

$$\sqrt{n_s}(|\widehat{g\pi}_{ij}|^2 - |g\pi_{ij}|^2) \rightarrow \mathcal{N}(0, \gamma^2), \quad (8)$$

where n_s is the number of observations and

$$\gamma^2 = \mathbf{g}_\alpha \mathcal{C} \boldsymbol{\Omega}_\alpha \mathcal{C}^T \mathbf{g}_\alpha^T + \mathbf{g}_w \boldsymbol{\Omega}_w \mathbf{g}_w^T, \quad (9)$$

for

$$\mathbf{g}_\alpha = 2 \frac{\mathbf{a}^T \mathbf{I}_{ij}^c \mathbf{S}^{-1} \mathbf{I}_{ij}^c \mathbf{a}}{\mathbf{a}^T \mathbf{I}_j^c \mathbf{S}^{-1} \mathbf{I}_j^c \mathbf{a}} - 2 \frac{\mathbf{a}^T \mathbf{I}_{ij}^c \mathbf{S}^{-1} \mathbf{I}_{ij}^c \mathbf{a}}{(\mathbf{a}^T \mathbf{I}_j^c \mathbf{S}^{-1} \mathbf{I}_j^c \mathbf{a})^2} \mathbf{a}^T \mathbf{I}_j^c \mathbf{S}^{-1} \mathbf{I}_j^c \quad (10)$$

and

$$\mathbf{g}_w = \left[\frac{1}{\mathbf{a}^T \mathbf{I}_j^c \mathbf{S}^{-1} \mathbf{I}_j^c \mathbf{a}} [(\mathbf{I}_{ij}^c \mathbf{a})^T \otimes (\mathbf{a}^T \mathbf{I}_{ij}^c)] - \frac{\mathbf{a}^T \mathbf{I}_{ij}^c \mathbf{S}^{-1} \mathbf{I}_{ij}^c \mathbf{a}}{(\mathbf{a}^T \mathbf{I}_j^c \mathbf{S}^{-1} \mathbf{I}_j^c \mathbf{a})^2} [(\mathbf{I}_j^c \mathbf{a})^T \otimes (\mathbf{a}^T \mathbf{I}_j^c)] \right] \boldsymbol{\xi} \boldsymbol{\Theta}_K \quad (11)$$

for $\boldsymbol{\xi} = -\text{diag}(\text{vec}(\mathbf{S}^{-2}))$, $\boldsymbol{\Theta}_K = (\mathbf{T}_{2K,K} \otimes \mathbf{I}_{2K^2})(\mathbf{I}_K \otimes \text{vec}(\mathbf{I}_{2K} \otimes \mathbf{I}_K))$ and $\mathbf{T}_{L,M}$ standing for the commutation matrix [11].

When the innovation covariance is known *a priori* or does not need to be estimated, the term $\mathbf{g}_w \boldsymbol{\Omega}_w \mathbf{g}_w^T$ in (5) is to be taken as zero.

B. Null Hypothesis Test

Under the null hypothesis

$$H_0 : |g\pi_{ij}|^2 = 0 \iff \mathbf{I}_j^c \mathbf{a} = \mathbf{0} \quad (12)$$

both (10) and (11) equal zero, and (8) no longer applies so that the next Taylor term becomes necessary [12] and is quadratic in $[\mathbf{a}^T \boldsymbol{\epsilon}^T]^T$ and weighted by one half of gPDC's Hessian at the point of interest with an $O(n_s^{-1})$ dependence. Via a device similar to that used in [8], one can show that

$$n_s (\mathbf{a}^T \mathbf{I}_j^c \mathbf{S}^{-1} \mathbf{I}_j^c \mathbf{a}) (|\widehat{g\pi}_{ij}|^2 - |g\pi_{ij}|^2) \xrightarrow{d} \sum_{k=1}^q l_k \chi_1^2 \quad (13)$$

where l_k are the eigenvalues of $\mathcal{D} = \mathbf{L}^T \mathbf{I}_{ij}^c \mathbf{S}^{-1} \mathbf{I}_{ij}^c \mathbf{L}$, where \mathbf{L} is the Choleski factor of $\bar{\boldsymbol{\Omega}} = \mathcal{C} \boldsymbol{\Omega}_\alpha \mathcal{C}^T$. Furthermore $q = \text{rank}(\mathcal{D}) \leq 2$, its value is 1 whenever $\lambda \in \{0, \pm 0.5\}$ and when the model order $p = 1$ for all $\lambda \in [-0.5, 0.5]$.

The result in (13) amounts to a linear combination of χ_1^2 variables whose relative weights depend on estimated parameter and covariance values.

IV. NUMERICAL ILLUSTRATIONS

A. Simulated data

To illustrate the present asymptotic $g\text{PDC}$ results, we simulated the five-channel toy model we originally introduced in [1] and a variant of its formulation as proposed by [13] repeated here for reference,

$$\begin{cases} x_1(t) = .95\sqrt{2}x_1(t-1) - .9025x_1(t-2) \\ \quad + e_1(t) + a_1e_6(t) + b_1e_7(t-1) + c_1e_7(t-2) \\ x_2(t) = .5x_1(t-2) \\ \quad + e_2(t) + a_2e_6(t) + b_2e_7(t-1) + c_2e_7(t-2) \\ x_3(t) = -.4x_1(t-3) \\ \quad + e_3(t) + a_3e_6(t) + b_3e_7(t-1) + c_3e_7(t-2) \\ x_4(t) = -.5x_1(t-2) + .25\sqrt{2}x_4(t-1) + .25\sqrt{2}x_5(t-1) \\ \quad + e_4(t) + a_4e_6(t) + b_4e_7(t-1) + c_4e_7(t-2) \\ x_5(t) = -.25\sqrt{2}x_4(t-1) + .25\sqrt{2}x_5(t-1) \\ \quad + e_5(t) + a_5e_6(t) + b_5e_7(t-1) + c_5e_7(t-2) \end{cases}$$

containing additionally a large exogenous input $e_6(t)$ and a latent variable $e_7(t)$. In the simulations $e_i(t)$ were uncorrelated zero mean unit variance Gaussian white noise and the variables were chosen $a_i \sim U(0, 1)$, $b_i = 2$ and $c_i = 5$, $i = 1, \dots, 5$ as in [13]. Also for reference, $n_s = 2,000$ data points were used and the results are represented as using unit sample frequency. Application of the Akaike information criterion (AIC) produced model orders $p = 3$ on most runs.

1) *Toy model without extra variables:* Using Monte Carlo simulations (2,000 runs), the original toy model excluding extra exogenous/latent terms produced results consistent with the asymptotic computations depicted in Fig. 1.

2) *Toy with exogenous/latent variables:* To provide an assessment of the impairment that the extra exogenous/latent variables might have on the null hypothesis thresholds associated with (13) we repeated the procedure under the same conditions of [13]. A typical run can be appreciated in Fig. 2 which stands in sharp contrast to the results in [13] who claim that PDC is inadequate when extra exogenous/latent variables are present. It is perhaps useful to note that correct connectivity patterns could still be obtained even if the original PDC were being used [13]. The reader may check our statement by employing and examining the open access MATLAB code for both PDC and $g\text{PDC}$ provided at www.lcs.poli.usp.br/~baccala/pdc.

The observed departure from the theoretical asymptotic distribution for nonexistent connection observed in Fig. 3B is in accord with the increase of false positives to roughly 7.8%

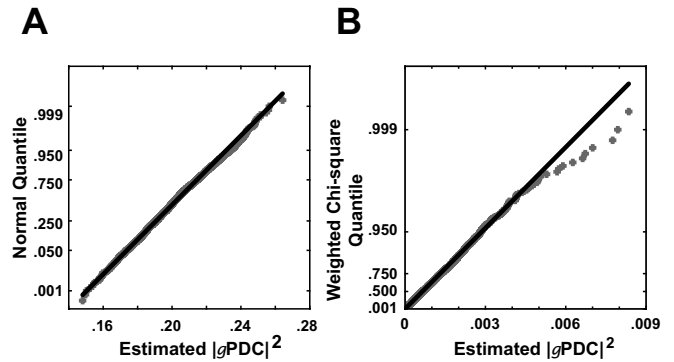


Fig. 1. Quantile $|g\text{PDC}|^2$ s plots (2,000 runs) and their theoretical distributions for the model in Sec. (IV-A) without exogenous and latent variables for computed at $\lambda = 0.2$ the normal plot for the existing connection $x_1 \rightarrow x_4$ (A), contrasted to the absent direct connection $x_1 \rightarrow x_5$ (B), the $|g\pi_{15}(0.2)|^2$ distribution is compared to the quantiles of two properly weighted chi-squares, producing good fits in both cases.

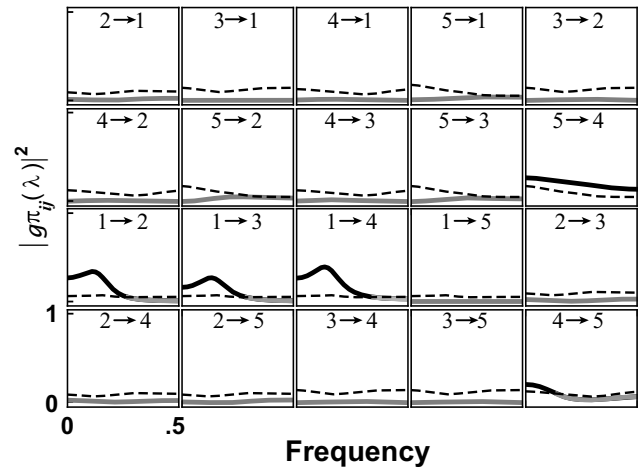


Fig. 2. Typical $|g\text{PDC}|^2$ run outcome between all channel pairs for the complete toy model in Sec. (IV-A) using the same plot layout in [13] to facilitate comparison. The thick lines on plots $1 \rightarrow 2$, $1 \rightarrow 3$, $1 \rightarrow 4$, $4 \rightarrow 5$ and $5 \rightarrow 4$ are above 1% $|g\text{PDC}|^2$ threshold and correctly estimated the connectivity pattern of the model. The frequency dependent thresholds are represented by dashed lines whereas light gray lines stand for $|g\text{PDC}|^2$'s whose nullity could not be rejected.

when $\alpha = 1\%$ is used to detect nonexistent connections. Approximately 4% false negatives, mostly associated with the $x_4 \rightarrow x_5$ connection, were observed. The false positive rate dropped to about 1% upon removal of the exogenous input/latent variables from (IV-A).

B. Real data with limited samples

To probe asymptotic test validity we analyzed a well known data set borrowed from [14] relating the melanoma incidence in the state of Connecticut and the Wölfer sunspot number measured from 1936 to 1972 (37 time points). Both time series were detrended before analysis. The common sense notion that the number of observed melanoma cases cannot possibly influence solar activity was confirmed and the sun's role in the disease vindicated (see Fig. 4) as the latter is above threshold as opposed to the former. This is an interesting result considering how small n_s is even at $\alpha =$

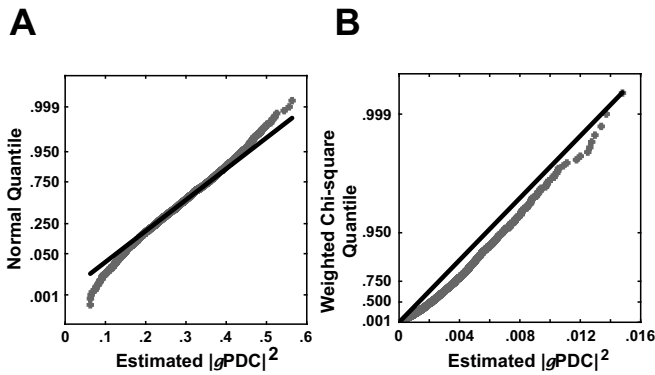


Fig. 3. $|gPDC|^2$ s quantile plots (2,000 runs) portraying the perturbation caused by including the exogenous and latent variables in the toy model at $\lambda = 0.2$. The existing connection $x_1 \rightarrow x_4$ remains practically Gaussian (A), whereas one observes a systematic deviation for the absent direct connection $x_1 \rightarrow x_5$ (B) which can explain the increase in false positive cases compared to the toy model without the extra variables. In the simulations the following values were adopted: $a_1 = 0.59$; $a_2 = 0.52$; $a_3 = 0.72$; $a_4 = 0.98$ and $a_5 = 0.66$.

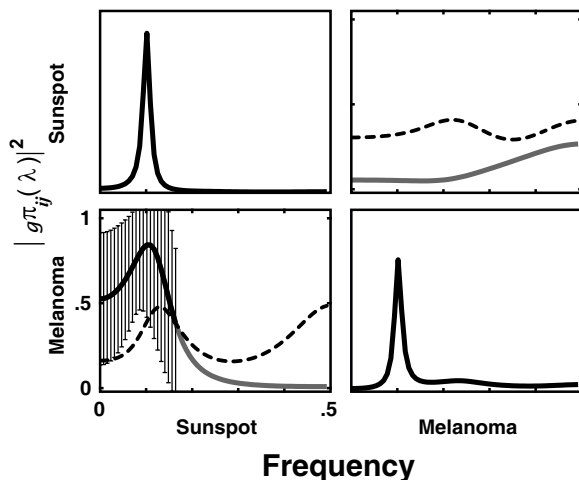


Fig. 4. The $|gPDC|^2$ and power spectra between sunspot and detrended Connecticut melanoma incidence 1936-1972 time series. The autospectra are on the main diagonal in arbitrary units. The black thick line in the Sunspot \rightarrow Melanoma $|gPDC|^2$ panel indicates above the 1% asymptotic threshold (dashed line) is surrounded by vertical bars to indicate the 99% $|gPDC|^2$ estimate confidence interval. Below threshold $|gPDC|^2$ is represented by a gray line. Note the peak of $|gPDC|^2$ coincides with Sunspot and Melanoma series power spectra peaks which correspond to an approximate 11 year-cycle period. Threshold value dependence on frequency is clear as well as in Fig. 2.

1%. Also interesting is the fact that test thresholds obtained via bootstrap statistics with 5,000 repetitions, see [15], of the inferred VAR model lead to an average 25% higher threshold in the melanoma to solar activity case without significantly altering the actually observed false alarm rates.

V. FINAL COMMENTS

After a brief recap of the definition of generalized partial directed coherence, a useful frequency domain connectivity measure between time series, its asymptotic confidence intervals and null hypothesis rejection were provided.

The asymptotic results were gauged via Monte Carlo simulations that showed good large sample fit and robustness even in the presence of exogenous/latent variables.

By applying the results to real data with just a few data samples, we provided evidence of the utility of $gPDC$'s asymptotics in detecting directed connectivity even under such adverse conditions thereby opening the way for $gPDC$'s rigorous use in practical applications.

VI. ACKNOWLEDGMENTS

The authors acknowledge support from the FAPESP Grant 2005/56464-9 (*CInAPCe*). C.S.N.B. to CAPES fellowship. D.Y.T. to fellowships from CAPES and FAPESP Grant 2008/08171-0. L.A.B to CNPq Grants 306964/2006-6 and 304404/2009-8.

REFERENCES

- [1] L. A. Baccalá and K. Sameshima, "Partial directed coherence: a new concept in neural structure determination." *Biol. Cybern.*, vol. 84, no. 6, pp. 463–474, 2001.
- [2] J. S. Bendat and A. G. Piersol, *Random Data: Analysis and Measurement Procedures*. Wiley, New York, 1986.
- [3] C. W. J. Granger, "Investigating causal relations by econometric models and cross-spectral methods." *Econometrica*, vol. 37, no. 3, pp. 424–438, 1969.
- [4] M. Steriade, D. A. McCormick, and T. J. Sejnowski, "Thalamocortical oscillations in the sleeping and aroused brain." *Science*, vol. 262, no. 5134, pp. 679–685, 1993.
- [5] G. G. Supp, A. Schlögl, N. Trujillo-Barreto, M. M. Müller, and T. Gruber, "Directed cortical information flow during human object recognition: analyzing induced EEG gamma-band responses in brain's source space." *PLoS One*, vol. 2, no. 1, p. e684, 2007.
- [6] A. J. Cadotte, T. H. Mareci, T. B. DeMarse, M. B. Parekh, R. Rajagovindan, W. L. Ditto, S. S. Talathi, D.-U. Hwang, and P. R. Carney, "Temporal lobe epilepsy: anatomical and effective connectivity." *IEEE Trans. Neural Syst. Rehabil. Eng.*, vol. 17, no. 3, pp. 214–223, 2009.
- [7] J. R. Sato, D. Y. Takahashi, S. M. Arcuri, K. Sameshima, P. A. Moretin, and L. A. Baccalá, "Frequency domain connectivity identification: an application of partial directed coherence in fMRI." *Hum. Brain. Mapp.*, vol. 30, no. 2, pp. 452–461, 2009.
- [8] D. Y. Takahashi, L. A. Baccalá, and K. Sameshima, "Connectivity inference between neural structures via partial directed coherence." *J. Appl. Stat.*, vol. 34, no. 10, pp. 1259–1273, 2007.
- [9] L. A. Baccalá, D. Y. Takahashi, and K. Sameshima, "Generalized partial directed coherence," in *15th International Conference on Digital Signal Processing*, 2007, pp. 163–166.
- [10] A. W. van der Vaart, *Asymptotic Statistics*. Cambridge University Press, Cambridge, 1998.
- [11] H. Lutkepöhl, *New Introduction to Multiple Time Series Analysis*. Springer, New York, 2005.
- [12] R. J. Serfling, *Approximation Theorems of Mathematical Statistics*. Wiley, New York, 1980.
- [13] S. Guo, J. Wu, M. Ding, and J. Feng, "Uncovering interactions in the frequency domain." *PLoS Comput. Biol.*, vol. 4, no. 5, p. e1000087, 2008.
- [14] D. F. Andrews and A. M. Herzberg, *Data: A Collection of Problems from Many Fields for the Student and Research Worker*. Springer, New York, 1985.
- [15] L. A. Baccalá, D. Y. Takahashi, and K. Sameshima, *Handbook of Time Series Analysis*. Wiley-VCH, Weinheim, 2006, ch. Computer intensive testing for the influence between time-series, pp. 411–435.